



Study of $K^+ \rightarrow \pi^0 e^+ \nu \gamma$ decay with OKA setup

A. Yu. Polyarush^{1,a}, **S. A. Akimenko**², **A. V. Artamonov**², **A. M. Blik**², **V. S. Burtovoy**², **V. N. Bychkov**³, **S. V. Donskov**², **V. A. Duk**^{1,4}, **A. P. Filin**², **S. N. Filippov**¹, **A. M. Gorin**², **E. N. Gushchin**¹, **A. V. Inyakin**², **G. D. Kekelidze**³, **G. V. Khaustov**², **S. A. Kholodenko**², **A. A. Khudyakov**¹, **V. N. Kolosov**², **V. I. Kravtsov**¹, **Yu. G. Kudenko**^{1,5,6}, **V. F. Kurshetsov**², **V. A. Lishin**², **V. M. Lysan**³, **M. V. Medynsky**², **Yu. V. Mikhailov**², **V. F. Obraztsov**², **V. A. Polyakov**², **V. I. Romanovsky**², **V. I. Rykalin**², **A. S. Sadovsky**², **V. D. Samoilenco**², **M. M. Shapkin**², **O. V. Stenyakin**², **O. G. Tchikilev**², **V. A. Uvarov**², **O. P. Yushchenko**², **B. Zh. Zalikhanov**³

¹ Institute for Nuclear Research of the Russian Academy of Sciences, 117312 Moscow, Russia

² “NRC Kurchatov Institute-IHEP”, 142281 Protvino, Russia

³ Joint Institute of Nuclear Research, 141980 Dubna, Russia

⁴ Present address: INFN-Sezione di Perugia, Via A. Pascoli, 06123 Perugia, Italy

⁵ National Research Nuclear University (MEPhI), Moscow, Russia

⁶ Institute of Physics and Technology, Moscow, Russia

Received: 25 October 2020 / Accepted: 19 January 2021 / Published online: 16 February 2021

© The Author(s) 2021

Abstract Results of a study of the $K^+ \rightarrow \pi^0 e^+ \nu \gamma$ decay at OKA setup are presented. More than 32,000 events of this decay are observed. The differential spectra over the photon energy and the photon–electron opening angle in kaon rest frame are presented. The branching ratios, normalized to that of K_{e3} decay are calculated for different cuts on E_γ^* and $\cos\Theta_{e\gamma}^*$. In particular, the branching ratio for $E_\gamma^* > 30$ MeV and $\Theta_{e\gamma}^* > 20^\circ$ is measured $R = \frac{Br(K^+ \rightarrow \pi^0 e^+ \nu_e \gamma)}{Br(K^+ \rightarrow \pi^0 e^+ \nu_e)} = (0.587 \pm 0.010(\text{stat.}) \pm 0.015(\text{syst.})) \times 10^{-2}$, which is in a good agreement with ChPT $O(p^4)$ calculations.

1 Introduction

The decay $K^+ \rightarrow \pi^0 e^+ \nu \gamma$ provides fertile testing ground for the Chiral Perturbation Theory (ChPT) [1, 2], an effective field theory of the QCD at low energies.

$K^+ \rightarrow \pi^0 e^+ \nu \gamma$ decay was first considered in [3] up to the order ChPT $O(p^4)$ and branching ratios were evaluated for given cuts on the photon energy and in the photon–electron opening angle in the kaon rest frame: $E_\gamma^* > E_\gamma^{cut}$, $\Theta_{e\gamma}^* > \Theta_{e\gamma}^{cut}$. Later the ChPT analysis was revisited and extended to $O(p^6)$ plus QED radiative corrections [4]. The branchings at tree level were also calculated in papers [5, 6], as well as T-odd correlations which are important in searches for the New Physics(NP).

The matrix element for $K^+ \rightarrow \pi^0 e^+ \nu \gamma$ decay has general structure

$$T = \frac{G_F}{\sqrt{2}} e V_{us} \epsilon^\mu(q) \left\{ (V_{\mu\nu} - A_{\mu\nu}) \bar{u}(p_\nu) \gamma^\nu (1 - \gamma_5) v(p_e) + \frac{F_\nu}{2p_e q} \bar{u}(p_\nu) \gamma^\nu (1 - \gamma_5) (m_e - \hat{p}_e - \hat{q}) \gamma_\mu v(p_e) \right\} \equiv \epsilon^\mu A_\mu.$$

The first term of the matrix element describes the bremsstrahlung of kaon and the direct emission. $A_{\mu\nu}$ contains WZW Chiral anomaly. The relevant diagram is displayed in Fig. 1a. The lepton bremsstrahlung is presented by the second part of Eq. (1) and Fig. 1b. The hadronic tensors $V_{\mu\nu}^{had}$ and $A_{\mu\nu}^{had}$ are defined by

$$I_{\mu\nu} = i \int d^4 e^{iqx} \langle \pi^0(p') | T V_\mu^{em}(x) I_\nu^{had}(0) | K^+(p) \rangle,$$

$I = V, A$, with $V_\nu^{had} = \bar{s} \gamma_\nu u$, $A_\nu^{had} = \bar{s} \gamma_\nu \gamma_5 u$, $V_\mu^{em} = (2\bar{u} \gamma_\mu u - \bar{d} \gamma_\mu d - \bar{s} \gamma_\mu s)/3$ and F_ν is the K^+_{e3} matrix element $F_\nu = \langle \pi^0(p') | V_\nu^{had}(0) | K^+(p) \rangle$.

The bremsstrahlung part of the amplitude is largely dominant in the partial decay width. Only with the advent of high statistics kaon decay experiments it become feasible to study effects of structure-dependent contributions and of the chiral anomaly.

The numerical results given in [3–6] demonstrate that non-trivial ChPT effects can be detected by the experiment. This gives a motivation for the present study.

^a e-mail: Polyarush@inr.ru (corresponding author)

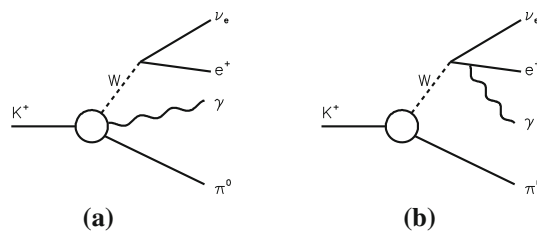


Fig. 1 Diagrams describing $K^+ \rightarrow \pi^0 e^+ \nu_e \gamma$ decay

2 OKA setup

The OKA collaboration operates at the IHEP Protvino U-70 Proton Synchrotron. The OKA detector (see Fig. 2) is located at the positive High Radio Frequency (RF) separated beam with 12.5% of kaons with a momentum of 17.7 GeV/c and an intensity of $3 \cdot 10^5$ kaons per 2 sec U-70 spill. RF-separation with the Panofsky scheme is realized. It uses two superconductive Karlsruhe-CERN Super Conductive RF deflectors [7], donated by CERN. A sophisticated cryogenic system, built at IHEP [8] provides superfluid He for the cavities cooling. The detailed description of the OKA detector is given in our previous publications [9, 10].

The OKA is taking data since 2010. In this study, we use the statistics that was collected in the 2012 and 2013 years. The total number of kaons entering the Decay Volume (DV) corresponds to $\sim 3.4 \times 10^{10}$.

A rather simple trigger was used during data-taking:

$\text{Tr} = S_1 \cdot S_2 \cdot S_3 \cdot S_4 \cdot \check{C}_1 \cdot \check{C}_2 \cdot \overline{S}_{bk} \cdot (E_{GAMS} > 2.5 \text{ GeV})$. $S_1 - S_4$ are scintillating counters; \check{C}_1, \check{C}_2 – Cherenkov counters (\check{C}_1 sees pions, \check{C}_2 pions and kaons); S_{bk} – two scintillation counters on the beam axis after the magnet to suppress undecayed particles.

The Monte Carlo (MC) simulation of the OKA setup is done within the GEANT3 framework [11]. Signal and

background events are weighted according to corresponding matrix elements.

3 Event selection and background suppression

Criteria for event selection:

1. One positive charged track detected in the tracking system and four showers detected in the electromagnetic calorimeters GAMS-2000 and BGD.
2. One shower must be associated with the charged track.
3. The charged track is identified as a positron. The positron identification is done using the ratio of the energy of the shower in GAMS-2000 to the momentum of the associated track. The E/p distribution is shown in Fig. 3. The particles with $0.8 < E/p < 1.2$ are accepted as positrons. Another cut used for the suppression of the π^+ contamination is that on the distance between the charged track extrapolation to the front plane of the electromagnetic detector and the nearest shower. This distance must be less than 3 cm.
4. The decay vertex situated within the decay volume.
5. The mass $M_{\gamma\gamma}$ of the $\gamma\gamma$ – pair closest to the Table value of π^0 is $0.12 < M_{\gamma\gamma} < 0.15 \text{ GeV}$. The energy of a photon originated from π^0 is greater than 0.5 GeV. The energy of the radiative photon is greater than 0.8 GeV. The absence of signals in the veto system above the noise threshold is also required.

The main background decay channels for the decay $K^+ \rightarrow \pi^0 e^+ \nu_e \gamma$ are:

1. $K^+ \rightarrow \pi^0 e^+ \nu$ with an extra photon. The main source of extra photons is positron interactions in the detector.
2. $K^+ \rightarrow \pi^+ \pi^0 \pi^0$ where one of the π^0 photons is not detected and π^+ is misidentified as a positron.

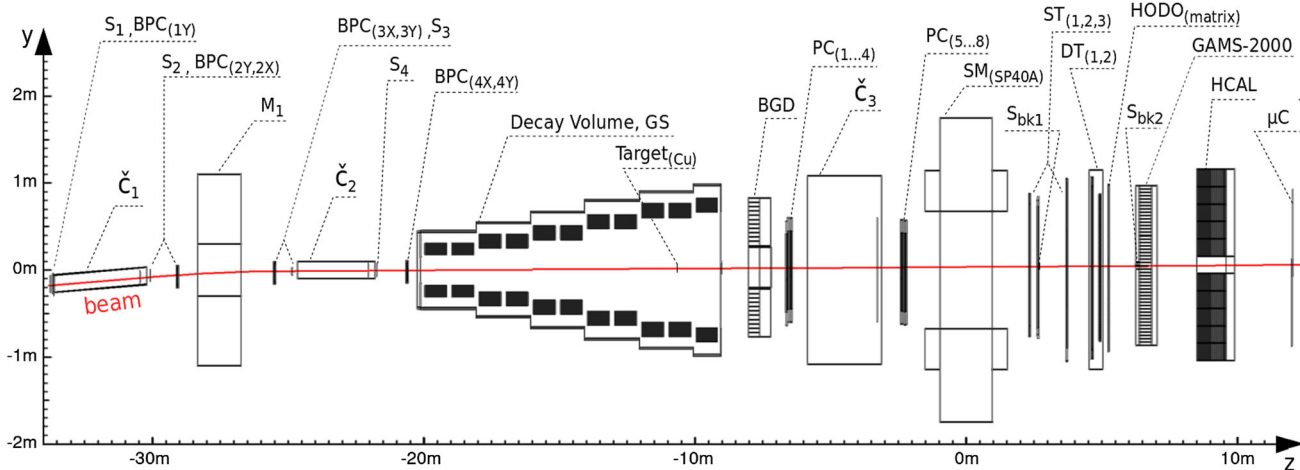


Fig. 2 Layout of the OKA detector, reproduced from [10]

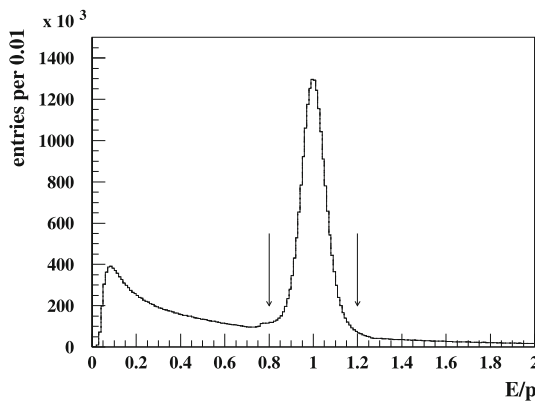


Fig. 3 E/p ratio for the real data

3. $K^+ \rightarrow \pi^+ \pi^0$ with a “fake photon” and π^+ misidentified as a positron. The fake photon clusters can come from πn interaction in the gamma detector and from accidentals.
4. $K^+ \rightarrow \pi^+ \pi^0 \gamma$ when π^+ is mis-identified as a positron.
5. $K^+ \rightarrow \pi^0 \pi^0 e^+ \nu$ when one γ is lost.

All these background sources are included in our MC calculations.

To suppress the background channels we use a set of cuts:

Cut 1: $E_{\text{miss}} = E_{\text{beam}} - E_{\text{detected}} > 0.5 \text{ GeV}$. The requirement on the missing energy mainly reduces the background (4).

Cut 2: $\Delta y = |y_\gamma - y_e| > 5 \text{ cm}$, where y is the vertical coordinate of a particle in the electromagnetic calorimeter (the magnetic field turns charged particles in the xz-plane).

Cut 3: $|x_\nu, y_\nu| < 100 \text{ cm}$. The reconstructed missing momentum direction must cross the active area of the electromagnetic calorimeter.

Cut 4: $M_{K \rightarrow \pi^0 e^+ \nu_e \gamma} > 0.45 \text{ GeV}$. $M_{K \rightarrow \pi^0 e^+ \nu_e \gamma}$ – the reconstructed mass of the $(\pi^0 e^+ \nu_e \gamma)$ -system, assuming $m_\nu = 0$. To enforce this cut we use a requirement on the missing mass squared $M_\nu^2 = (P_K - P_{\pi^0} - P_e - P_\gamma)^2$. For the signal events this variable corresponds to the square of the neutrino mass and must be zero within measurement accuracy.

Cut 5: $-0.003 < M_\nu^2 < 0.003 \text{ GeV}^2$.

The dominant background to $K_{e3\gamma}$ arises from K_{e3} with an extra photon (background (1)). This background is suppressed by a requirement on the angle between positron and photon in the laboratory frame $\Theta_{e\gamma}$ (see Fig. 4). The distribution of the $K_{e3\gamma}$ background events has a very sharp peak at zero angle. This peak is significantly narrower than that for the signal events. This happens, in particular, because the emission of the photons by the positron

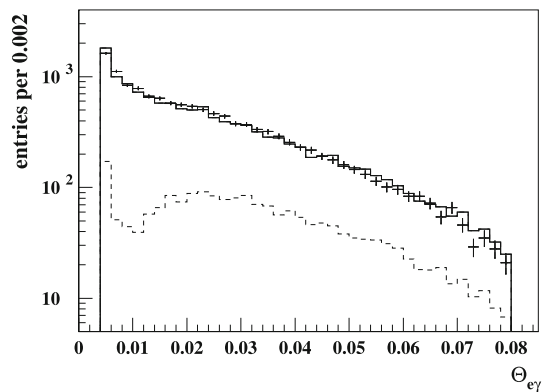


Fig. 4 The distribution over $\Theta_{e\gamma}$ – the angle between positron and photon in lab. system. Real data (points with errors), signal plus MC background (solid line histogram), MC background (dotted line histogram)

occurs in the setup material downstream the decay vertex, but the angle is still calculated as if emission comes from the vertex.

Cut 6: $0.004 < \Theta_{e\gamma} < 0.080 \text{ rad}$. The left part of this cut is introduced exactly for the suppression of background (1). The right cut is against $K_{\pi 2}$ background.

After all the cuts, 32676 candidates are selected, with a background of 4624 events. Background normalization is done by comparison of the number of events for K_{e3} decay in MC and real data samples.

4 Results

The resulting distribution of the selected events over $\cos(\Theta_{e\gamma}^*)$, $\Theta_{e\gamma}^*$ being the angle between the positron and the photon in the kaon rest frame, is shown in Fig. 5. Some discrepancy between data and MC is seen in two right bins of Fig. 5, related to that in two first bins of Fig. 4. The effect of this mismatch on the results is minimized by the cut on $\cos(\Theta_{e\gamma}^*)$ (see below).

The distribution over E_γ^* – the photon energy in the kaon rest frame is shown in Fig. 6. Reasonable agreement of the data with MC is seen. When generating the signal MC, a generator based on $O(p^4)$ calculations [3] is used.

To obtain the branching ratio for the $K_{\pi^0 e^+ \nu_e \gamma}$ relative to the K_{e3} (R), the background and efficiency corrected number of $K_{e3\gamma}$ events is normalized on that of about 9M K_{e3} events found with similar selection criteria.

The relative branching ratio (R) for the soft cuts $E_\gamma^* > 10 \text{ MeV}$ and $\Theta_{e\gamma}^* > 10^\circ$ is found to be

$$R_1 = (1.990 \pm 0.017(\text{stat.}) \pm 0.021(\text{syst.})) \times 10^{-2}.$$

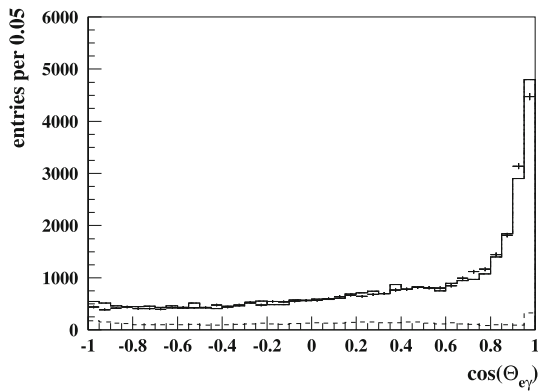


Fig. 5 The distribution of the events over $\cos\Theta_{e\gamma}^*$. Points with errors are the real data, histogram – MC signal plus background, MC background – dotted line histogram

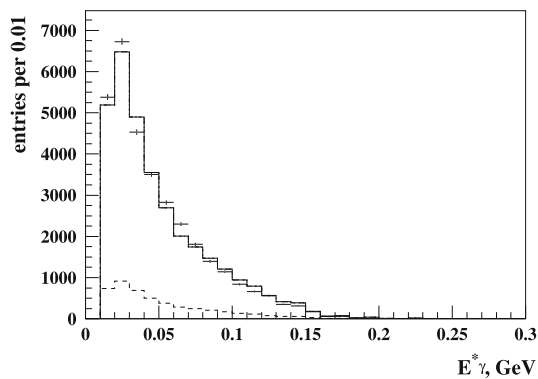


Fig. 6 The distribution of the events over E_{γ}^* . Points with errors – the real data, histogram – MC signal plus background, MC background – dotted line histogram

And for the cuts $E_{\gamma}^* > 30$ MeV and $\Theta_{e\gamma}^* > 20^\circ$ used in the most theoretical papers

$$R_2 = (0.587 \pm 0.010(stat.) \pm 0.015(syst.)) \times 10^{-2}$$

For the comparison with previous experiments the branching ratio with the cuts $E_{\gamma}^* > 10$ MeV, $0.6 < \cos\Theta_{e\gamma}^* < 0.9$ is calculated

$$R_3 = (0.532 \pm 0.010(stat.) \pm 0.012(syst.)) \times 10^{-2}$$

The main systematic errors are estimated by variation of the cuts 1–6. Contributions of each cut variation to systematic errors are given in Table 1. Some other sources of systematics, like trigger effects and effects of the MC model were investigated and found to be negligible.

The comparison with previous experiments is given in Table 2.

Table 1 Contributions to systematic errors

R_i	1	2	3	4	5	6
R_1	0.003	0.002	0.006	0.008	0.015	0.011
R_2	0.004	0.001	0.004	0.005	0.010	0.008
R_3	0.001	0.001	0.005	0.001	0.010	0.004

Table 2 $\text{Br}(K^+ \rightarrow \pi^0 e^+ \nu_e \gamma)/\text{Br}(K^+ \rightarrow \pi^0 e^+ \nu_e)$ for $E_{\gamma}^* > 10$ MeV, $0.6 < \cos\Theta_{e\gamma}^* < 0.9$ in comparison with previous data

$R_3 \times 10^2$	N_{ev}	Experiment
$0.53 \pm 0.01 \pm 0.01$	7248	This experiment
$0.48 \pm 0.02 \pm 0.03$	1423	ISTRa+ [12, 13]
0.46 ± 0.08	82	XEBC [14, 15]
0.56 ± 0.04	192	ISTRa [16–18]
0.76 ± 0.28	13	HLBC [19]

5 Conclusions

The largest statistics of about 32K events of $K_{e3\gamma}$ is collected by the OKA experiment. The relative branching ratio $R = \text{Br}(K^+ \rightarrow \pi^0 e^+ \nu_e \gamma)/\text{Br}(K^+ \rightarrow \pi^0 e^+ \nu_e)$ is measured for different cuts on the photon energy and the photon–electron angle in the kaon rest frame. The obtained value of R for $E_{\gamma}^* > 30$ MeV and $\Theta_{e\gamma}^* > 20^\circ$ is in a good agreement with the ChPT $O(p^4)$ prediction [3] $R = (0.592 \pm 0.005) \times 10^{-2}$ and is some $2\text{--}3\sigma$ away from the tree level results [5, 6]. The $O(p^6)$ result [4] is 2.5σ higher. That is, the measurement becomes sensitive to the non-trivial ChPT effects and perhaps to the NP effects.

Acknowledgements The authors express their gratitude to the colleagues from the accelerator department for good performance of the U-70 during data taking; to colleagues from the beam department for the stable operation of the 21K beam line, including RF-deflectors, and to colleagues from the engineering physics department for the operation of the cryogenic system of the RF-deflectors. The work is supported in part by the Russian Foundation for Basic Research, Grant N18-02-00179A.

Data Availability Statement This manuscript has no associated data or the data will not be deposited. [Authors' comment: OKA data will be released after the intended period of operation, and corresponding publication of results.]

Open Access This article is licensed under a Creative Commons Attribution 4.0 International License, which permits use, sharing, adaptation, distribution and reproduction in any medium or format, as long as you give appropriate credit to the original author(s) and the source, provide a link to the Creative Commons licence, and indicate if changes were made. The images or other third party material in this article are included in the article's Creative Commons licence, unless indicated otherwise in a credit line to the material. If material is not included in the article's Creative Commons licence and your intended use is not permitted by statutory regulation or exceeds the permitted use, you will need to obtain permission directly from the copyright holder. To view a copy of this licence, visit <http://creativecommons.org/licenses/by/4.0/>

[ons.org/licenses/by/4.0/](https://creativecommons.org/licenses/by/4.0/).

Funded by SCOAP³.

References

1. S. Weinberg, Phys. A **96**, 327 (1979)
2. J. Gasser, H. Leutwyler, Nucl. Phys. B **250**, 465 (1985)
3. J. Bijnens, G. Ecker, J. Gasser, Nucl. Phys. B **396**, 81 (1993)
4. B. Kubis et al., Eur. Phys. J. C **50**, 557 (2007)
5. V.V. Braguta, A.A. Likhoded, A.E. Chalov, Phys. Rev. D **65**, 054038 (2002)
6. I.B. Khriplovich, A.S. Rudenko, Phys. Atom. Nucl. **74**, 1214 (2011)
7. A. Citron et al., Nucl. Instrum. Methods Phys. Res. **164**, 31 (1979)
8. A. Ageev et al., *Proceedings of the Particle Accelerator Conference* (RuPAC, Zvenigorod, 2008), p. 282
9. A.S. Sadovsky et al., Eur. Phys. J. C **78**, 92 (2018).
[arXiv:1709.01473](https://arxiv.org/abs/1709.01473) [hep-ex]
10. M.M. Shapkin et al., Eur. Phys. J. C **79**, 296 (2019).
[arXiv:1808.09176](https://arxiv.org/abs/1808.09176) [hep-ex]
11. R. Brun et al. CERN-DD/EE/84-1
12. V.N. Bolotov et al., Yad. Fiz. **70**, 1 (2007)
13. V.N. Bolotov et al., Phys. Atom. Nucl. **70**, 29 (2007)
14. V.V. Barmin et al., SJNP **53**, 606 (1991)
15. V.V. Barmin et al., Yad. Fiz. **53**, 981 (1991)
16. V.N. Bolotov et al., JETP Lett. **42**, 68 (1986)
17. V.N. Bolotov et al., Yad. Fiz. **44**, 108 (1986)
18. V.N. Bolotov et al., Sov. J. Nucl. Phys. **44**, 68 (1986)
19. F. Romano et al., Phys. Lett. B **36**, 525 (1971)